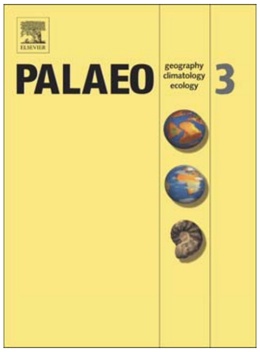

Quantification of climate change for the last 20,000 years from Wonderkrater, South Africa: implications for the long-term dynamics of the Intertropical Convergence Zone

Loïc Truc, Manuel Chevalier, Charly Favier, Rachid Cheddadi, Michael E. Meadows, Louis Scott, Andrew S. Carr, Gideon F. Smith, Brian M. Chase

PII: S0031-0182(13)00301-5
DOI: doi: 10.1016/j.palaeo.2013.06.024
Reference: PALAEO 6548

To appear in: *Palaeogeography, Palaeoclimatology, Palaeoecology*

Received date: 6 March 2013
Revised date: 14 June 2013
Accepted date: 21 June 2013

Please cite this article as: Truc, Loïc, Chevalier, Manuel, Favier, Charly, Cheddadi, Rachid, Meadows, Michael E., Scott, Louis, Carr, Andrew S., Smith, Gideon F., Chase, Brian M., Quantification of climate change for the last 20,000 years from Wonderkrater, South Africa: implications for the long-term dynamics of the Intertropical Convergence Zone, *Palaeogeography, Palaeoclimatology, Palaeoecology* (2013), doi: 10.1016/j.palaeo.2013.06.024

Quantification of climate change for the last 20,000 years from Wonderkrater, South Africa: implications for the long-term dynamics of the Intertropical Convergence Zone

Loïc Truc*[1], Manuel Chevalier[1], Charly Favier[1], Rachid Cheddadi[1], Michael E. Meadows[2], Louis Scott[3], Andrew S. Carr[4], Gideon F. Smith[5,6,7], Brian M. Chase[1, 8]

[1] Institut des Sciences de l'Evolution de Montpellier, UMR 5554, Centre National de Recherche Scientifique/Université Montpellier 2, Bat.22, CC061, Place Eugène Bataillon, 34095 Montpellier, cedex5, France;

[2]Department of Environmental and Geographical Science, University of Cape Town, Private Bag X3, Rondebosch 7701, South Africa;

[3]Department of Plant Sciences, University of the Free State, Bloemfontein 9300, South Africa;

[4]Department of Geography, University of Leicester, Leicester, LE1 7RH, UK;

[5]Office of the Chief Director: Biosystematics Research and Biodiversity Collections, South African National Biodiversity Institute, Private Bag X101, Pretoria 0001 South Africa;

[6]Schweickerdt Herbarium, Department of Botany, University of Pretoria, Pretoria, 0002 South Africa;

[7]Centre for Functional Ecology, Departamento de Ciências da Vida, Universidade de Coimbra, 3001-455 Coimbra, Portugal

[8]Department of Archaeology, History, Culture and Religion, University of Bergen, Postbox 7805, 5020, Bergen, Norway

**corresponding author: loic.truc@univ-montp2.fr*

Highlights

- Quantitative estimates of climate at a key South African site over the past 20 kyr.
- Reconstructed trends show strong links with regional sea-surface temperatures.
- Reconstructions indicate interhemispheric synchrony in the African tropics.
- Findings do not support the hypothesis of direct insolation forcing of tropical African climates.
- Highlights a promising technique for analyzing palaeobotanical data in the region.

Abstract

In a region for which few palaeoenvironmental records are available, the fossil pollen record from the Wonderkrater spring mound has contributed substantially to our understanding of past vegetation changes in southeast Africa since the Last Glacial Maximum (LGM; 21 ka). Principal component analyses of the pollen data by Scott and Thackeray (1987) provided environmental reconstructions suggesting relatively mesic LGM conditions, with warm and dry conditions during the early Holocene (11-6 cal kBP). This conforms to predicted patterns of precipitation change in the southern African tropics in response to Northern Hemisphere cooling and orbital forcing. Subsequent data from the Cold Air Cave speleothems and a sea-surface temperature record from the Mozambique Chanel, however, indicate that conditions during the early to mid-Holocene may have been wetter than present in the Wonderkrater region. To explore this question further, we have created a series of botanical-climatological transfer functions based on a combination of modern climate and plant distribution data from southern Africa. Applying these to the Wonderkrater fossil pollen sequence, we have derived quantitative estimates for temperatures during the cold and warm quarters, as well as precipitation during the wet and dry quarters. In addition, a species-selection method based on Bayesian statistics is outlined, which provided a parsimonious choice of likely plant species from what are otherwise taxonomically broad pollen-types.

We do not propose that our findings invalidate the previous principal component analyses, but they do have the advantage of being based more clearly on the relationship between modern plant distributions and individual climatic variables. Results indicate that temperatures during both the warm and cold season were 6±2°C colder during the Last Glacial Maximum and Younger Dryas, and that rainy season precipitation during the Last Glacial Maximum was ~50% of that during the mid-Holocene. Our results also imply that changes in precipitation at Wonderkrater generally track changes in Mozambique Channel sea-surface temperatures, with a steady increase following the Younger Dryas to a period of maximum water availability at Wonderkrater ~3-7 ka. These findings argue against a dominant role of a shifting Intertropical Convergence Zone in determining long-term environmental trends, and indicate that the northern and southern tropics experienced similar climatic trends during the last 20 kyr.

Keywords: Quaternary, southern Africa, pollen analysis, transfer function, probability density function, quantitative climate reconstruction, African Humid Period, Intertropical Convergence Zone

Introduction

Late Quaternary climate variability in the Southern Hemisphere is a matter of significant debate, with a range of hypotheses invoking different forcing climatic mechanisms to explain observed patterns of change. In the southern tropics and subtropics of Africa, the most commonly posited phenomenon is latitudinal adjustment in the mean annual position of the Intertropical Convergence Zone (ITCZ). This is potentially driven by high latitude Northern Hemisphere cooling (e.g. Flohn, 1981; Johnson et al., 2002) and/or direct insolation forcing (e.g. Braconnot et al., 2008; COHMAP, 1988; Kutzbach, 1981; Liu et al., 2003; Marzin and Braconnot, 2009). Both hypotheses imply an inter-hemispheric anti-phase relationship, that is, aridification in northern tropics would be expected to coincide with humidification in the southern tropics (Scott, 1993; Street-Perrott and Perrott, 1993; Partridge et al. 1997; Scott et al. 1997; Schefuß et al., 2011). To date, however, no irrefutable evidence supporting either hypothesis has been found in southern Africa (cf. Chase et al., 2010).

In this context, southern Africa is a key region in which to investigate vegetation and climate dynamics, which may support, modify or falsify hypotheses concerning the Quaternary dynamics of the ITCZ. The region is highly sensitive to perturbations in the Earth's climate system, both at regional and global scales (cf. Chase and Meadows, 2007; Dupont et al., 2011) due to its position at the juncture of temperate, subtropical and tropical climate systems. However, this region is also characterised by a lack of reliable, well-dated proxy records, and palaeoecological evidence is particularly sparse and often difficult to interpret.

One record that has played a particularly important role in shaping our understanding of past vegetation changes in southeast Africa during the late Quaternary is the fossil pollen sequence from the Wonderkrater spring mound (Scott, 1982; Scott, 1999; Scott and Thackeray, 1987; Thackeray, 1999). Notably, the record has been interpreted as indicating a cool, but moist, Last Glacial Maximum (LGM)/last glacial-interglacial transition (LGIT) and a dry early Holocene (Scott et al., 1987 ; Scott et al., 2003). These findings support both the hypothesis of a southward shift of the ITCZ due to

Northern Hemisphere cooling and that of direct insolation forcing in response to precessional changes in the Earth's orbit.

As other records have been obtained from the region, however, certain paradoxes have become evident in the aggregate regional dataset. For example, high resolution stable isotope records from the Cold Air Cave speleothem spanning the last 25 kyr imply that the early to mid-Holocene was more humid than the LGM at Wonderkrater (Holmgren et al., 2003; Lee-Thorp et al., 2001). More recently, a longer, but lower resolution pollen record for the last 340 kyr from off the Limpopo River mouth suggests that warmer periods are generally more humid in the region (Dupont et al., 2011). The physical mechanism for this is thought to be the strong positive relationship between sea-surface temperatures (SSTs) in the Mozambique Channel (Caley et al., 2011; Sonzogni et al., 1998) and continental humidity in eastern South Africa, both under present conditions (Goddard and Graham, 1999), and over multi-millennial timescales (Chase et al., 2010; Dupont et al., 2011), with warmer SSTs favouring increased evaporation and moisture transport. A question therefore arises as to whether the principal components extracted from the Wonderkrater pollen sequence discretely reflect temperature and humidity, as has been proposed.

The aim of this paper is to develop a new approach for interpreting the pollen data and investigate this paradox, in order to improve our understanding of the forcing mechanisms driving regional climate variability since the LGM. To explore this question, we use plant distribution and climate data to define the specific climatic requirements of the plant taxa comprising the primary pollen-types in the Wonderkrater sediment core, and to develop botanical-climatological transfer functions based on probability density functions (*pdf*s). As well as addressing a critical topic in southern African palaeoclimatology, this paper also describes the methods by which quantitative, rather than qualitative, estimates of past climatic parameters can be obtained from southern African fossil pollen records. This represents a significant step in this region, and it promises to provide the basis for more robust comparisons of palaeoenvironmental data and general circulation model simulations.

Study area and regional settings

This study primarily considers trends in past vegetation and climate in the vicinity of the Wonderkrater spring mound (24.4390°S, 28.7507°E) in northeastern South Africa. However, the transfer function techniques applied necessitate a broader analysis of the distribution of plant taxa across southern Africa, including South Africa, Lesotho, Swaziland, Botswana and Namibia (17° - 34°S and 11° - 32°E) (Figure 1). The wider study area is characterized by strong heterogeneity in terms of its topography, geology and climate. The complexity of this landscape, and the oceanic and atmospheric circulation systems that determine the region's climate have resulted in strong environmental gradients that have a clear influence on plant distributions.

Considering southern Africa as a whole, precipitation is associated with two major circulation systems, *viz*: (1) tropical systems, including easterly flow from the Indian Ocean and northwesterly flow from the tropical Atlantic Ocean. These develop with seasonal heating of the continent, both of which are related to annual migrations of the ITCZ; (2) temperate systems, which influence the region as frontal systems embedded in the westerly storm-track that migrates equatorward in winter months (cf. Chase and Meadows, 2007) (Figure 2). Mean annual rainfall ranges from c. 800 mm per annum in south east South Africa, to <50 mm per annum in Namibia. Isohyets are orientated in a broadly east-west manner in more tropical latitudes, but become increasingly north-south orientated in central and south-west South Africa, which reflects the increasing significance of the mid-latitude anticyclones and temperate systems relative to the Intertropical Convergence Zone (ITCZ) in driving atmospheric (in)stability and rainfall patterns (cf. Tyson and Preston-Whyte, 2000). The alternating seasonal dominance of these systems therefore results in a strong seasonality gradient in precipitation across the subcontinent, manifested as a summer rainfall zone in the eastern part of the sub-continent (SRZ, >66% of mean annual precipitation falling between Oct-Mar), a winter rainfall zone in the southwest (WRZ, >66% of mean annual precipitation falling between Apr-Sept) and a transitional zone sometimes referred to as the year-round rainfall zone (YRZ), which receives both winter and summer precipitation (cf. Chase and Meadows, 2007). Both of these broad climate regions are highly variable in terms of temperature and precipitation, with mean annual values ranging from 6.5°C - 24.4°C and

10 - 1380 mm yr^{-1} in the SRZ, and 10.8°C - 19.9°C and 25 - 970 mm yr^{-1} in the WRZ (Hijmans et al., 2005).

At local and region scales both temperature and precipitation are strongly influenced by topography, and the diversity of vegetation types is also influenced by edaphic conditions. Generally, vegetation in the SRZ is composed of a variety of subtropical savannas, shrublands, grasslands and woodland (Rutherford & Westfall, 1994). In contrast, the WRZ is associated with mediterranean shrublands (known as fynbos and renosterveld).

The Wonderkrater site is located within the SRZ (Figure 2), with mean annual rainfall of ~550 mm. It is characterised by wet summers (DJF; ~285 mm) and very dry winters (JJA; ~15 mm) (data from Hijmans et al., 2005). Mean seasonal temperatures are 23°C and 13.5 C° during summer and winter respectively. The vegetation at the site is part of the Central Bushveld known as the Springbokvlakte Thornveld (Mucina and Rutherford, 2006). This vegetation is an open to dense savannah dominated by various species of *Acacia* or shrubby grassland. Important trees and shrubs include *Acacia karroo*, *A. leuderitzii*, *A. mellifera*, *A. nilotica*, *Ziziphus mucronata*, *Boscia foetida*, *B. albitrunca*, *Euclea undulata*, *Searsia* (*Rhus*) *engleri*, *Dichrostachys cinerea*, *Diospyros lycioides*, *Grewia flava* and *Tarchonanthus camphoratus*, while the grasses are primarily comprised of *Aristida bipartita*, *A. canescens*, *Dicanthium annulatum*, *Iscaenum afrum*, *Setaria incrassata* and *Brachiaria eruciformis* (Mucina and Rutherford, 2006).

Data and methods

Southern Africa is subject to important constraints in terms of quantitative palaeoclimate reconstruction methodologies. For example, transfer function techniques such as the mutual climatic range method (MCR) (Atkinson et al., 1986; Fauquette et al., 1998; Grichuk, 1969, 1984), which determines the climatic range of fossil floras by combining the mutual climatic envelope of the pollen-types in assemblages, is unsuited to regions of high biodiversity, such as southern Africa (Birks & Seppa, 2004). This results from the fact that while the vegetation itself is highly diverse, the pollen taxonomy is only able to differentiate to familial or generic levels. As such, identifiable pollen-types can encompass a wide range of taxa, among which there may be several species with different or even contrasting climatic requirements. This results in broad – sometimes multimodal – climatic envelopes, and unrealistic climatic optima (Klotz et al., 2003). Another technique, the modern analogues technique (MAT) (Guiot, 1990), which is based on the comparison of fossil pollen spectra with their modern equivalents, cannot yet be applied in southern Africa as a suitable collection of modern pollen samples has not yet been developed for the region. Traditional regression methods such as WA (weighted averaging) and WA-PLS (weighted averaging - partial least squares) cannot, therefore, be employed as there are insufficient data to calibrate regression models (Braak and Juggins, 1993).

In this context, we have developed a transfer function based on probability density functions (*pdf*s), (Kühl et al., 2002), which are calculated from known plant species distributions. This reconstruction method uses a sub-set of dominant pollen types and from modern distribution data identifies the most appropriate climate variables influencing their distribution. The most parsimonious choice of species included in each fossil pollen type is identified as a function of the assemblage as a whole for a given time step. This method is capable of not only providing quantitative estimates of palaeoclimatic variables, but it can in many cases also discern more clearly seasonal variability in rainfall and temperature, which is of paramount importance in southern Africa.

Botanical, climatic and fossil pollen data

Botanical data were extracted from a series of databases held by the South African National Biodiversity Institute (http://sibis.sanbi.org/faces/DataSources.jsp; Rutherford et al., 2012; Rutherford et al., 2003; SANBI, 2003). These data, which are derived mainly from herbarium collections, but also from observations, are in general available as ‘presence’ within a particular quarter degree (0.25° × 0.25°) grid square, and we have thus adopted this as the resolution for our analyses, upscaling more precisely located data to this common resolution.

In order to define plant species distributions as a function of climate, we have used climatic variables from WORLDCLIM1.4 (Hijmans et al., 2005), which, along with monthly precipitation and temperature data, provides a dataset of 19 bioclimatic variables that are considered important elements in studying the eco-physiological tolerance of plants species. Some of these bioclimatic variables are, however, highly correlated with each other, introducing information redundancy which can be misleading when analysing the relative contribution of each variable. In order to choose a set of weakly correlated descriptors that most appropriately explain plant species distributions, we calculated the correlation between these 19 bioclimatic variables. Ultimately, this led to the retention of four variables, *viz.* precipitation during the driest quarter (of the year) (PDryQ), precipitation of the wettest quarter (PWetQ), mean temperature of the warmest quarter (TWarmQ), and mean temperature of the coldest quarter (TColdQ) (Figure 3). These four variables represent groups of correlated variables that are thought to play distinct, significant roles in plant species distribution. These data were then upscaled to the same resolution as the botanical data (0.25°).

From the fossil record recovered from Wonderkrater, we selected 19 pollen taxa according to their prevalence in the record and/or their importance as palaeoenvironmental indicators, as identified by Scott (1982; 1999), Scott and Thackeray (1987) and Scott et al. (2003) (Table 1). The taxonomic resolution of our analyses is the same as for the fossil pollen analysis. For each of these taxa, all the species represented by ten or more occurrences have been extracted from the SANBI database.

The chronologic control for the Wonderkrater sediment cores has been problematic (primarily as a result of root contamination (cf. Scott et al., 2003)). While older samples exist from the site, we have excluded them, restricting our analysis to samples from Borehole 3, the chronology of which is based on the ages selected by Scott for this sequence (Scott et al., 2003). These have been recalibrated here using the SHCal04 calibration dataset (McCormac et al., 2004) for Holocene ages and the IntCal09 calibration dataset (Reimer et al., 2009) for older ages. The age-depth model (Figure 4) and individual sample ages were calculated based on linear interpolation using the R script "Clam" of Blaauw et al. (2010). Considering the dating uncertainties associated with the Wonderkrater sequence, the timing of the events and trends described for this site should still, however, be treated as best estimates.

Resolving climatic influence over species distribution

To define the most important modern climatic variables controlling the distribution of the 19 pollen taxa selected from the Wonderkrater record (Table 1), we used the Maxent species distribution modelling method (Phillips et al., 2006) using Maxent 3.3.3k. This method is well-suited to presence data only (Elith, 2006)requiring only species presence data and climatic variable layers. From these it estimates the probability of a species' occurrence in a given grid cell as a function of the climatic variables provided. The model's performance was classically evaluated by partitioning the dataset, with 70% of the samples being randomly chosen for model fitting and 30% for model testing. The models' performances were estimated by the AUC (Area Under the Curve) of the ROC curve (Receiver Operating Characteristic). The ROC curve provides a quantitative representation of the tradeoffs between no omission (sensitivity) and commission errors (1-specificity). The area under the ROC curve (AUC) is an important measure of the model performance and yields an index ranging in value from 0 to 1. A good model ranges from 0.8 to 1 (Swets, 1988).

Finally, we quantified the contribution of each climatic variable in the models using the jackknife contribution method, which calculates the contribution of each variable in two types of models, *viz*. one involving only a given variable, and the other involving all variables except that given variable (cf. Phillips et al., 2006). AUC calculated on the full model and these two models provides evidence as to which climatic variables contribute most to the full model.

Pollen-climate transfer function

Here we present an alternative methodology using a botanical-climatological transfer function based on *pdf*s calculated from the geographical distribution of the species included in each selected pollen type (Table 1). For this, we assume the existence of a functional relationship between climate and plant species distribution, and that this relationship has not changed over the time period in question.

The establishment of this transfer function is determined by the following steps (summarized in Figure 5):

(1) Results from the Maxent modelling process are used to identify the most important climatic variables determining a pollen type's distribution, and to choose the sensitive set of pollen types for the reconstruction of each climatic variable. For this reconstruction, we retained only pollen types where the variable contribution is higher than 10% (Table 1).

(2) We calculate the likelihood of a climatic variable (x) given the presence of a pollen type (y). $\mathcal{L}(x|y)$ is the conditional probability of presence pollen type (y) given the value of (x): $P(y|x)$ as follows:

$$(1) \quad \mathcal{L}(x|y) = P(y|x) = \frac{f(x|y)P(y)}{f(x)}$$

Where $f(x)$ is the *pdf* of the climatic variable x in the study area, $f(x|y)$ is the *pdf* of the variable *x* where species *y* is present and $P(y)$ is the probability of presence of species *y* (prevalence).

To ensure that *pdf*s reflect the plant-climate relationship rather than the climatic space of the study area, we used the weighting method developed in Kühl et al (2002). This method aims at rebalancing climate dataset according to the occurrence of a given climate space in the study area. The use of this method for temperature variables results in a shift of the climatic optimum toward the class of values that are at the limits of the climatic space, and are thus represented by fewer cells, but for which the cells are always occupied by the plants (Figure 6).

In contrast to the reconstruction of temperature variables, the distribution of PDryQ and PWetQ does not demand such weighting. As opposed to an increase in temperature, an increase in precipitation is less likely to be a limiting factor as the ecophysiological tolerance of plants to high precipitation is greater than for temperature. Such cells are occupied more frequently even for plants showing dry optima, and the use of this weighting method leads to over estimates of the climate values over this threshold, leading to unrealistic *pdf*s.

(3) An assemblage (*k*) is defined as the set of present pollen type: $k = \{y_i\}$. Assuming that the occurrence of pollen types are independent events, the likelihood of a climatic variable (*x*) given the assemblage (*k*) is:

$$(2)\quad \mathcal{L}(x|k) = \prod_{y_i \in k} \mathcal{L}(x|y_i)$$

(4) We calculate the likelihood of a climatic variable (x) given the presence of each species included in each pollen type (y). $\mathcal{L}(x|y)$ is the conditional probability of presence species (y) given the value of (x): $P(y|x)$ and is computed by:

$$(3)\quad \mathcal{L}(x|y) = P(y|x) = \frac{f(x|y)P(y)}{f(x)}$$

Where $f(x)$ is the *pdf* of the climatic variable (x) in the study area, $f(x|y)$ is the pdf of the variable (x) where species (y)is present and $P(y)$ is the probability of presence of species (y).

(5) We calculate the probability that a given species (*y*) is included in the *pdf* of the assemblage (*k*), given the climatic variable (x) involved as follows:

$$(4)\quad \Pr(y|k)_j = \int (pdf(y|x).pdf(x|k)_j).dx$$

We have removed all species whose probability of presence in the fossil assemblage, based on the climatic variables influencing their distribution (Table 1) is lower than 20% for any given time-step. This threshold was chosen, in consideration of the large climatic envelopes of many species, to avoid the inclusion of species that might reflect substantially different climatic tolerances. In this procedure, the *pdf*s of the assemblage are recalculated in the same way; removing other species and reducing the range of the climatic envelope for the assemblage as a whole. Generally, after three repetitions of this process the number of species stabilizes and the process is stopped. Finally, we get the new *pdfs*, generated from the distribution of the pollen-types composed of species with probability of presence in the assemblage is higher than 20%.

(6) The last step is to calculate the reconstructed climatic values independently of each other, based on the maximum value (optima) of the *pdf*s of each pollen type including those species that are most likely to be present in a given assemblage. Thereafter, this value (*z*) is weighted by the pollen

percentage (normalized by their maximum percentage values; *p*) and averaged to calculate the weighted mean value (*w*) for an assemblage (*k*) as follows:

$$(5) \quad W_k = \frac{\sum z_i \cdot p_i}{\sum p_i}$$

In our approach, we assume that (1) normalized pollen percentage reflects the relative abundance of a given taxon in the vicinity of the site, and (2) that a relationship exists between the climatic optima of these taxa and the observed pollen percentage (Birks & Seppä, 2004).

RESULTS

Resolving the influence of climate on species distribution

Results from modelling indicate the role of selected climatic variables on the distribution of the selected pollen types identified in the Wonderkrater record (Table 1). The results indicate: 1) the pollen types used to reconstruct each palaeoclimatic variable, 2) the climatic variables that have the greatest influence on their distributions, and 3) whether the pollen types are favoured by high or low values of a given climatic variable. For our discussion, the selected pollen types have been divided into three groups of associated elements, as a function of their climatic requirements.

Response of fynbos elements

Fynbos elements are represented by Proteaceae, Ericaceae, *Cliffortia*, *Passerina* and *Stoebe*-type pollen. All these taxa are major components of the Fynbos Biome (Figure 2) of the Cape Floristic Region (CFR) (Cowling et al., 1997), but they also occupy a wide spatial and climatic range. Their distribution forms an arc encompassing several biomes, from the CFR through the montane grasslands of the Drakensberg and Highveld to the savannas of northeastern South Africa.

Modelling results for these elements shows that their geographical distribution is influenced primarily by temperature, with fynbos elements being mainly restricted to areas where TWarmQ is below 23°C and TColdQ is above 10°C. These variables indicate that the temperature during the wettest quarter (which is associated with the TWarmQ in the Savannah Biome and TColdQ in Fynbos

Biome) plays a dominant role on fynbos taxa distribution. For the reconstruction of TWarmQ and TColdQ, all fynbos elements were used.

In terms of rainfall, precipitation during the growing season corresponds to PColdQ in the Fynbos Biome (WRZ) and the PWarmQ in the Savannah Biome (SRZ). For the Fynbos pollen types these two variables are expressed in PWetQ, which shows a bimodal distribution ranging from 50 to 700 mm (except for in the case of *Stoebe*-type) reflecting the weak influence of this variable on the distribution of fynbos taxa. The response of these taxa to PWetQ can be explained by their distribution across the WRZ, YRZ and SRZ, with the bimodal distribution reflecting 1) the climate of the Fynbos Biome and particularly the WRZ (PWetQ of 170 mm when averaged over the whole of the biome), and 2) climate in the Savannah Biome, where the rainfall during the wet season is generally higher. Importantly, this is particularly so at higher altitudes where these taxa are found in the SRZ. However, even if a few species can be separated geographically in these two modes, the majority are found along the length of the continuum from the CFR to the savannah. We have not, therefore used fynbos elements to reconstruct precipitation (with the exception of *Stoebe*-type taxa, which indicate generally low PWarmQ in the Wonderkrater region).

Response of savannah elements

Savannah elements include Combretaceae, *Burkea*, *Acacia*, *Tarchonanthus*, Capparaceae and *Spirostachys.* The results show that the distributions of these taxa are affected by both precipitation and temperature. In terms of PWetQ, Combretaceae, *Spirostachys* and *Burkea* show strong, unimodal requirements, with optima at 350±90 mm. Capparaceae and *Tarchonanthus,* however, display a more complex response to PWetQ. For this variable, these taxa occupy a wide range (0 to 700 mm), which indicates high variability in terms of the requirements of the individual species included in these pollen types.

These particular taxa are however less diverse than others considered here, and it is possible to consider the individual species included within each pollen type. The genus *Tarchonanthus*, for example, is currently represented in the Wonderkrater region (within 500 km) by *T. trilobus*, *T. parvicapitulatus* and *T. camphoratus.* The first two species show similar PWetQ requirements around

350±90 mm, while *T. camphoratus* requires less precipitation, and can occupy areas where PWetQ is relatively low (170±110 mm). Capparaceae can also be divided into two groups of species, differentiated by their rainfall regime, except for a few cosmopolitan species, which can be found in the two groups. Unlike fynbos elements, where the majority of species can be found in the two modes, the bimodal distribution of *Tarchonanthus* and Capparaceae can be directly attributed to differences in individual species requirements. Such inter-specific variability can be anticipated to lead to complications in the interpretation of the palaeoclimatic significance of their pollen.

In our analysis we have applied a species selection method, focusing on the climatic requirements of individual species, which allowed us to make a parsimonious choice among the species included in each pollen type as a function of the assemblage as a whole. Of the Capparaceae species found in the Wonderkrater region today, thirteen have a probability of being found in the assemblage during the early Holocene less than 0.2 (Figure 7b). When we remove these species from the Capparaceae pollen type we get a new optimum value that is more realistic and coherent with the pollen assemblage. Similarly, while one of the species of *Tarchonanthus* (*T. camphoratus)* is an important element in the dry savannah, the three others (*T. trilobus*, *T. parvicapitulatus* and *T. litoralis*) are found in regions that are currently as wet or wetter than Wonderkrater. The species selection method indicates that *T. camphoratus* was less likely to have been present during the early Holocene (0.31), and the increase of *Tarchonanthus* pollen during this period was most likely due to an increase of taxa such as *T. trilobus* (0.79), *T. parvicapitulatus* (0.83) and *T. litoralis* (0.49). Together, these results allow a refinement of the taxa identification, and the interpretation of the pollen record. While the reconstructed first order variability is similar both before and after species selection is carried out (Figure 8), the species selection method allows for a more refined reconstruction, particularly during the early Holocene, which appears to be more consistent with changes in the dominant regional forcing mechanisms (see Discussion).

Modelling results indicate that the distribution of savannah elements is also sensitive to warmer temperatures. Combretaceae, Capparaceae and *Acacia* represent the taxa which require the highest TWarmQ values (optima = 25±2.3°C). To conclude, savannah elements can be considered as strong indicators of warm and wet summer (PWetQ) environments with a marked winter dry season (PDryQ).

Response of other elements

This diverse group comprises taxa showing relationships between their distribution and climate that cannot be readily incorporated into either the fynbos or savannah groupings. They do, however, show significant change in their abundance in the Wonderkrater pollen record and as they are known to be important indicators of particular climatic conditions they have been included in our reconstructions.

Podocarpus is represented by four species in southern Africa. It is a drought intolerant afromontane forest element, whose distribution is mainly constrained by PDryQ (≥70±25 mm). This pollen type is considered to be an indicator of wet conditions, but our results suggest that its distribution is more specifically controlled by drought stress (sometimes facilitated by cool, but not cold, habitats (20±2.1°C optimum for TWarmQ)). The coastal and montane distribution of *Podocarpus* relates to the availability of sufficient moisture to support growth even during the dry season.

Anthospermum spp. show similar requirements to fynbos elements, whose distribution is influenced by TWarmQ. This taxon is however more cosmopolitan than other fynbos elements. At Wonderkrater, *Anthospermum* can therefore be considered as an indicator of cool conditions.

Chenopodiaceae is a very widespread family, inhabiting xeric and halophytic environments (Scott, 1982). Their distribution is mainly influenced by precipitation, occupying areas where PWetQ is relatively low. Consideration must, however, be given to the influence of agricultural irrigation and resultant changes in soil salinity on its modern distribution. Halophytes such as Chenopodiaceae may become important elements of the ecosystem when agricultural activities and irrigation lead to a salinisation of the soil (Rietz, 2003). This species can thus thrive as the result of local disturbance, but is also sensitive to regional changes in climate. For this study, we have not removed data points as a function of land use, but it may be that the strength of

Chenopodiaceae as an indicator of aridity has been attenuated by its association with relatively wet agricultural areas.

Aloe and *Euclea* are widespread genera whose distribution is mainly controlled by precipitation, generally occupying areas where PWetQ ≥ 400±180 mm. However, some species of *Aloe* and *Euclea,* can occupy extremely dry habitats, such as the Namib Desert and Succulent Karroo Biome (Smith & Van Wyk, 2008). In terms of temperature, some of these taxa (e.g. *Aloe polyphylla*) show strong resistance to low temperatures and can be found in the Drakensberg Mountains, where TColdQ can drop down to 1.5°C (Scott et al., 1987).

Olea is also strongly influenced by precipitation, with most species occupying areas where drought stress is limited (PDryQ ≥ 50±21 mm). An exception is *O. europaea* subsp. africana, which has been found in arid environments in Namibia, although generally along water courses.

Artemisia, mainly represented by *A. afra,* requires relatively low summer temperatures, and occupies chiefly the highveld or montane grasslands.

Quantitative palaeoclimatic reconstruction

Palaeo-temperatures

Using the data and techniques described above, we sought to develop the first quantitative pollen-based climatic reconstruction from southern Africa. To assess the performance of the transfer function, we first compared the reconstructed value from the top of the core, representing the modern - submodern assemblage with modern warm and cold season temperatures at Wonderkrater. The reconstructed temperatures (TWarmQ = 21.8±2.3°C, TColdQ = 13±2°C) are very close to actual values (TWarmQ = 22°C, TColdQ = 12.7°C).

Figures 9b and 9c show temperature reconstructions for the past 20 kyr derived from the Wonderkrater pollen data. These reconstructions show significant temperature variability, particularly across the LGIT, when TWarmQ rose from 18±1°C to 24±1.3°C and TColdQ rose from 9°±1°C to

15.5±1.2°C. Results show that the LGM was 6±2°C cooler than the mid-Holocene, and about 4±2°C cooler than present day. This can be seen in the high percentage of fynbos elements such as *Stoebe*, Ericaceae, Proteaceae, *Cliffortia* and *Passerina* in the pollen assemblages at this time, whose distribution, as indicated by the analysis here, will be strongly influenced by cooler climates.

Following Heinrich Stadial 1 (HS1; 18.5-14.6 ka) strong warming is observed in the record, from 13.6-12.5 cal kBP, approximately contemporaneous with the Bølling-Allerød (B/A). During this period, results show temperatures rising about 4°C relative to the LGM. In the pollen diagram, this period is characterised by a marked increase in savannah elements such as Combretaceae, *Tarchonanthus* and Capparaceae, accompanied by a steep decline in psycrophilic fynbos elements and dry indicators such as Chenopodiaceae. This relatively warm period is followed by cooling from 12.3 to 10.5 cal kBP, during which fynbos elements increase in abundance, and temperatures return to values similar to those of the LGM. The degree to which this cooling can be reliably attributed to the Younger Dryas (YD; 13-11.5 ka) event, observed elsewhere in southern Africa (Chase et al., 2011), is however, limited by the accuracy of the chronology of the Wonderkrater sequence (cf. Scott et al., 2003).

A gradual warming trend marks the beginning of the Holocene, with the model indicating maximum summer and winter temperatures occurring 8.3 - 6.5 cal kBP. Significant vegetation changes mark this phase, with the spread of savannah elements, especially *Tarchonanthus* and Capparaceae, and the decline of cool-climate taxa such as fynbos elements, which disappear completely in the pollen sequence during this period. After 6.5 cal kBP, we observed a sharp decrease of summer temperature from 23.8±1.5°C to 19.8±1.2°C. Following this major decline, temperatures are variable and show a complex pattern, oscillating between 21°C and 23°C to the present day.

Palaeo-precipitation

The reconstructed PWetQ value from the most recent pollen sample (260±25 mm; Figure 9e) does not correspond to contemporary rainfall at Wonderkrater (~310 mm; Hijmans et al., 2005). This discrepancy can perhaps be explained by either: 1) the increase in halophytic Chenopodiaceae (Figure

9g) as a result of irrigation activities during the phase of post-colonial vegetation disturbance, or 2) that the age-model based on the assumption of a modern age for the surface of the spring mound is inaccurate, and in fact the uppermost samples are somewhat older than previously thought, perhaps falling within a drier period.

These caveats notwithstanding, when the new analysis of the Wonderkrater record is considered as a whole, a clear and consistent positive relationship between temperature and precipitation throughout the last 20 kyr, with drier (wetter) conditions generally occurring during cooler (warmer) periods (Figure 9). The amplitude of summer rainfall variability is ~170 mm, with minimum values of ~150 mm during HS1 and the LGM and maximum values of ~320 mm from 7-3 cal kBP. Like the temperature record, the transition from LGM to the early Holocene is also characterized by two important phases. Following HS1, conditions rapidly become much wetter between 15-13.5 ka, with an increase in summer precipitation from ~150±25 to ~300±25 mm. It is interesting to note that the shift to wetter conditions seeming pre-dates the temperature increase in the Wonderkrater reconstruction by approximately 1000 years. In the pollen diagram, increased moisture availability is apparent from an increase in pollen from mesic savannah and thicket elements such as Combretaceae and *Aloe*, and a decrease in cool, relatively arid indicators such as *Stoebe*-type pollen. At ~12.3 cal kBP, summer precipitation declines sharply by ~125±25 mm, corresponding to the cooling in the palaeotemperatures reconstruction. This dry period is characterized by a reduction of pollen percentages from savannah and thicket elements, especially *Tarchonanthus*, Capparaceae and *Aloe*, and an increase in fynbos elements and Chenopodiaceae. However, while temperatures again lag, remaining low until ~10.5 cal kBP, warm season precipitation increases as early as ~11.5 cal kBP. This marks the beginning of a period of extended moisture that extends across the early and mid-Holocene, until ~2.9 cal kBP. The late Holocene is notably drier than today (30% lower PWetQ), but is also marked by significant variability, with some periods of wetter than present conditions.

DISCUSSION

Comparison with previous Wonderkrater reconstruction

The reconstructions presented here show that during the LGM summer temperatures at Wonderkrater were ~4±2°C lower than present and ~6±2°C lower than during the Holocene Altithermal. The difference is similar to previous estimates made on the basis of lapse rate between altitudes of savannah and fynbos belts in the region (Scott, 1982). The reconstructed LGM temperatures are similar to other temperature reconstructions for the sub-continent (Heaton et al., 1983; Kulongoski and Hilton, 2004; Stute and Talma, 1998; Talma and Vogel, 1992). For the duration of the record as a whole these results are very similar (r = 0.91) to the trends identified in the PCA-based reconstructions (Scott, 1999; Scott et al., 2012; Scott and Thackeray, 1987) (Figure 9). After 6.5 cal kBP, our reconstruction indicates greater variability than the PCAs; a difference that is probably due to the relatively low explained variance of axis 1 (14%), which suggests the influence of climatic variables other than temperature.

While the PCA-based reconstructions (Scott, 1999; Scott et al., 2012; Scott and Thackeray, 1987) and *pdf*-based temperature reconstructions from Wonderkrater show similar patterns, the reconstructions of palaeo-precipitation show significant differences (Figure 9). Interpretations of PCA axis 2 (PC2) suggested that the early Holocene (11 to 5.5 cal kBP) was significantly drier than the late Holocene (Scott, 1999; Scott and Thackeray, 1987). In contrast, our *pdf*-based reconstructions show an increase of moisture during the early Holocene. This important difference in results/interpretation may be related to the methodologies employed; specifically that the co-occurrence of taxa highlighted in PCAs may reflect the influence of a combination of environmental variables. While the co-variation of pollen type percentages is likely to have, at least to some degree, a basis in climatic variability, the attribution of humidity or temperature to a given axis can be more complicated. This may also explain why the explained PCA variance is relatively low (at Wonderkrater, axis 1 = 14%; axis 2 = 10%).

Considering the fossil pollen record (Figure 9g), it is evident that Capparaceae and *Tarchonanthus* pollen type drive the negative PC2 loading in the early Holocene. This finding, coupled with the dominance of these taxa in the vegetation of the bushveld and thornveld communities of the Kalahari dry savannah to the southeast of Wonderkrater (from which modern pollen assemblages from surfaces samples indicate the co-occurrence of *Tarchonanthus*, Capparaceae and *Aloe*, as observed in the fossil record) led Scott (1982; 1999) to interpret the second PCA axis as being strongly influenced by humidity. As mentioned, the species selection method we have applied allows us to focus on the climatic requirements of individual species, and make a parsimonious choice from the species included in each pollen type as a function of the assemblage as a whole. This analysis indicates that the more xeric taxa of *Tarchonanthus* and Capparaceae are less likely to have been present at the site during the early Holocene, further supporting the possibility that it may have been more humid than the PCAs indicate (Figures7 and 8).

It is interesting to note that strong positive correlations are observed between PC2 and our reconstructed values of PDryQ (Figure 9d/9e). Changes in PDryQ are negatively correlated with precipitation during the wet season across the Holocene (Figure 9f). This inverse trend could be interpreted as an increase in seasonality across this period, where rainfall was mainly restricted to summer wet season. The increase in precipitation during the wet season and decrease in the dry season observed in our results are driven by the appearance of savannah elements, including Combretaceae and *Burkea*, which require strong rainfall seasonality. The indication is that the relation between PDryQ and plants may not be directly related to precipitation amount, but rather reflect drought stress tolerance. The strong correlation between PC2 and PDryQ suggests that PC2 may be more a reflection of drought stress rather than rainfall amount.

The palaeoclimatic significance of Wonderkrater: a re-interpretation

The new reconstruction confirms previous estimates of the probable temperature depression associated with the LGM in southern Africa. It also provides some new insights into the magnitude of the climatic fluctuations associated with the period encompassing the last glacial-interglacial transition, a period for which there is increasing evidence of marked climatic dynamism in southern

Africa (e.g. Abel and Plug, 2000; Chase et al., 2011). For instance, these new data, although constrained by some chronological uncertainty suggest mean annual temperature fluctuations of an amplitude of c. 4°C during the LGIT, akin to the difference between current conditions and the LGM.

The *pdf*-based reconstructions of palaeo-precipitation coupled with new insights into the most likely species represented by the pollen types identified in the record allow us to also reconsider the meaning of PCA axis 2 in the original Wonderkrater analysis. A major finding of this new interpretation is that the early Holocene period in particular was associated with enhanced (rather than reduced) moisture availability, contrary to hypotheses that predict drier conditions concurrent with a austral summer insolation minimum (e.g. Braconnot et al., 2008; COHMAP, 1988; Kutzbach, 1981; Liu et al., 2003; Marzin and Braconnot, 2009). These new data closely mirror changes in Mozambique Channel SSTs (Sonzogni et al., 1998) (Figure 10g). They are consistent with expectations of increased continental moisture with in associated with elevated Indian Ocean SSTs (Chase et al., 2010; Dupont et al., 2011; Goddard and Graham, 1999; Stager et al., 2011).

From the wider region, lake high-stands at Lake Chilwa (Thomas et al., 2009) date to 12.8-13.7 ka and 15.4-16.1 ka, which coincides with the period of pronounced positive anomalies in SSTs in the Mozambique Channel (Sonzogni et al., 1998), as well as the more humid conditions now identified as following HS1 at Wonderkrater (Figure 10). Stable carbon isotope and greyscale records from nearby Cold Air Cave (Holmgren et al., 2003; Lee-Thorp et al., 2001) have been interpreted as indicating relatively humid conditions during the early to mid-Holocene, with increased tree cover (Lee-Thorp et al., 2001). To the north, markedly similar trends can be observed in the δ^{13}C records from the nearby Braamhoek wetland (Norstöm et al., 2009), marine core GeoB9307-3 (which we interpret to reflect vegetation cover in the Zambezi Basin, contrary to Schefuß et al., 2011), Lake Malawi (Castañeda et al., 2007), Lake Tanganiyka (Tierney et al., 2008) and even the distant site of Lake Challa (Sinninghe Damsté et al., 2011).

While a degree of regional variability is to be expected, and the shortcomings of the Wonderkrater chronologies must be kept in mind (cf. Scott et al., 2003), there is a strong coherence in the first order trends observed in these SE African records, with the YD, HS1 and LGM being generally drier, and the early to mid-Holocene being relatively humid (Figure 10). These combined findings support the hypothesis that deglacial increases in SW Indian Ocean SSTs played a fundamental role in determining continental climates in SE Africa (Stager et al., 2011) and that, while the mean latitudinal position of the ITCZ may have been displaced southward during periods of Northern Hemisphere cooling (Johnson et al., 2002; Schefuß et al., 2011), and northward as a response to direct insolation forcing during the early Holocene (Braconnot et al., 2007; Castañeda et al., 2007; Johnson et al., 2002; Kutzbach and Street-Perrott, 1985), these changes were secondary to primary responses to variations in evaporation and advection of moisture from the adjacent ocean.

Conclusions

- Our modelling approach allows us to better identify and constrain the influence of a range of climatic parameters on plant distributions, and thus create more robust, objective reconstructions.
- The species selection method developed in this paper allows the identification of the most parsimonious choice among species represented by specific pollen types, and is a useful tool in regions characterized by high biodiversity, particularly in southern Africa where taxonomic resolution have been a major constrain on palynological climatic reconstructions.
- This work suggests that the early Holocene may have been wetter than previous interpretations of the Wonderkrater record indicated and these new results exhibit strong correlations with SW Indian Ocean SSTs, as well as regional palaeoclimatic archives from several other locales, indicating a strong relationship between SST variability and continental humidity in SE Africa since the LGM.
- The new interpretation of this pollen sequence provides new quantitative information for the Late Pleistocene and Holocene, and improves our knowledge of the role and impact of various forcing mechanisms in the region, presenting a powerful tool for future palaeoclimatic reconstructions.

References

Abell, P.I., Plug, I., 2000. The Pleistocene/Holocene transition in South Africa: evidence for the Younger Dryas event. Global and Planetary Change 26, 173-179.

Atkinson, T.C., Briffa, K.R., Coope, G.R., Joachim, M.J., Perry, D.W., 1986. Climatic calibration of coleopteran data, In: B.E., B. (Ed.), Handbook of Holocene Palaeoecology and Palaeohydrology. Wiley, New York, pp. 851-859.

Berger, A., Loutre, M.F., 1991. Insolation values for the climate of the last 10 million years. Quaternary Science Reviews 10, 297-317.

Birks, H.J.B., Seppä, H., 2004. Pollen-based reconstructions of late-Quaternary climate in Europe–progress, problems, and pitfalls. Acta Palaeobotanica 44, 317-334.

Blaauw, M., 2010. Methods and code for `classical' age-modelling of radiocarbon sequences. Quaternary Geochronology 5, 512-518.

Braak, C.F., Juggins, S., 1993. Weighted averaging partial least squares regression (WA-PLS): an improved method for reconstructing environmental variables from species assemblages. Hydrobiologia 269-270, 485-502.

Braconnot, P., Marzin, C., Gregoire, L., Mosquet, E., Marti, O., 2008. Monsoon response to changes in Earth's orbital parameters: comparisons between simulations of the Eemian and of the Holocene. Clim. Past J1 - CP 4, 281-294.

Braconnot, P., Otto-Bliesner, B., Harrison, S., Joussaume, S., Peterchmitt, J.-Y., Abe-Ouchi, A., Crucifix, M., Driesschaert, E., Fichefet, T., Hewitt, C.D., Kageyama, M., Kitoh, A., Lâîné, A., Loutre, M.-F., Marti, O., Merkel, U., Ramstein, G., Valdes, P., Weber, L., Yu, Y., Zhao, Y., 2007. Results of PMIP2 coupled simulations of the Mid-Holocene and Last Glacial Maximum - Part 1: experiments and large-scale features. Climate of the Past 3, 261-277.

Brook, G.A., Scott, L., Railsback, L.B., Goddard, E.A., 2010. A 35 ka pollen and isotope record of environmental change along the southern margin of the Kalahari from a stalagmite and animal dung deposits in Wonderwerk Cave, South Africa. Journal of Arid Environments 74, 870-884.

Caley, T., Kim, J.H., Malaizé, B., Giraudeau, J., Laepple, T., Caillon, N., Charlier, K., Rebaubier, H., Rossignol, L., Castañeda, I.S., Schouten, S., Sinninghe Damsté, J.S., 2011. High-latitude obliquity as a dominant forcing in the Agulhas current system. Climates of the Past 7, 1285-1296.

Castañeda, I.S., Werne, J.P., Johnson, T.C., 2007. Wet and arid phases in the southeast African tropics since the Last Glacial Maximum. Geology 35, 823-826.

Chase, B.M., Meadows, M.E., 2007. Late Quaternary dynamics of southern Africa's winter rainfall zone. Earth-Science Reviews 84, 103-138.

Chase, B.M., Meadows, M.E., Carr, A.S., Reimer, P.J., 2010. Evidence for progressive Holocene aridification in southern Africa recorded in Namibian hyrax middens: implications for African Monsoon dynamics and the "African Humid Period". Quaternary Research 74, 36-45.

Chase, B.M., Quick, L.J., Meadows, M.E., Scott, L., Thomas, D.S.G., Reimer, P.J., 2011. Late glacial interhemispheric climate dynamics revealed in South African hyrax middens. Geology 39, 19-22.

COHMAP, 1988. Climatic changes of the last 18,000 years: observations and model simulations. Science 241, 1043-1052.

Cowling, R.M., Richardson, D.M., J., M.P., 1997. Fynbos, In: Cowling, R.M., Richardson, D.M., Pierce, S.M. (Eds.), Vegetation of Southern Africa. Cambridge University Press, Cambridge, pp. 99-130.

Dupont, L.M., Caley, T., Kim, J.H., Castañeda, I., Malaizé, B., Giraudeau, J., 2011. Glacial-interglacial vegetation dynamics in South Eastern Africa coupled to sea surface temperature variations in the Western Indian Ocean. Clim. Past 7, 1209-1224.

Elith, J., H. Graham, C., P. Anderson, R., Dudík, M., Ferrier, S., Guisan, A., J. Hijmans, R., Huettmann, F., R. Leathwick, J., Lehmann, A., Li, J., G. Lohmann, L., A. Loiselle, B., Manion, G., Moritz, C., Nakamura, M., Nakazawa, Y., McC. M. Overton, J., Townsend Peterson, A., J. Phillips, S., Richardson, K., Scachetti-Pereira, R., E. Schapire, R., Soberón, J., Williams, S., S. Wisz, M., E. Zimmermann, N., 2006. Novel methods improve prediction of species' distributions from occurrence data. Ecography 29, 129-151.

Fauquette, S., Guiot, J., Suc, J.-P., 1998. A method for climatic reconstruction of the Mediterranean Pliocene using pollen data. Palaeogeography, Palaeoclimatology, Palaeoecology 144, 183-201.

Flohn, H., 1981. A hemispheric circulation asymmetry during late Tertiary. Geologische Rundschau 70, 725-736.

Fauquette, S., Guiot, J., Suc, J.-P., 1998. A method for climatic reconstruction of the Mediterranean Pliocene using pollen data. Palaeogeography, Palaeoclimatology, Palaeoecology 144, 183-201.

Flohn, H., 1981. A hemispheric circulation asymmetry during late Tertiary. Geologische Rundschau 70, 725-736.

Gayo, E.M., Latorre, C., Jordan, T.E., Nester, P.L., Estay, S.A., Ojeda, K.F., Santoro, C.M., Late Quaternary hydrological and ecological change in the hyperarid core of the northern Atacama Desert (~ 21°S). Earth-Science Reviews.

Goddard, L., Graham, N.E., 1999. Importance of the Indian Ocean for simulating rainfall anomalies over eastern and southern Africa. J. Geophys. Res. 104, 19099-19116.

Grichuk, V.P., 1969. An attempt to reconstruct certain elements of the climate of the northern hemisphere in the Atlantic Period of the Holocene, In: Neishadt, M.I. (Ed.), Golotsen. Izd-vo Nauka, Moscow, pp. 41-57.

Grichuk, V.P., 1984. Late Pleistocene vegetation history, In: Velichko, A.A. (Ed.), Late Quaternary Environments of the Soviet Union. Longman, London, pp. 155-178.

Guiot, J., 1990. Methodology of the last climatic cycle reconstruction in France from pollen data. Palaeogeography, Palaeoclimatology, Palaeoecology 80, 49-69. Heaton, T.H.E., Talma, A.S., Vogel, J.C., 1983. Origin and history of nitrate in confined groundwater in the western Kalahari. Journal of Hydrology 62, 243-262.

Heaton, T.H.E., Talma, A.S., Vogel, J.C., 1983. Origin and history of nitrate in confined groundwater in the western Kalahari. Journal of Hydrology 62, 243-262.

Heaton, T.H.E., Talma, A.S., Vogel, J.C., 1986. Dissolved gas paleotemperatures and 18O variations derived from groundwater near Uitenhage, South Africa. Quaternary Research 25, 79-88.

Hijmans, R., Cameron, S.E., Parra, J.L., Jones, P.G., Jarvis, A., 2005. Very high resolution interpolated climate surfaces for global land areas. International Journal of Climatology 25, 1965-1978.

Holmgren, K., Lee-Thorp, J.A., Cooper, G.R.J., Lundblad, K., Partridge, T.C., Scott, L., Sithaldeen, R., Talma, A.S., Tyson, P.D., 2003. Persistent millennial-scale climatic variability over the past 25,000 years in Southern Africa. Quaternary Science Reviews 22, 2311-2326.

Johnson, T.C., Brown, E.T., McManus, J., Barry, S., Barker, P., Gasse, F., 2002. A high-resolution paleoclimate record spanning the past 25,000 years in southern East Africa. Science 296, 113-132.

Kulongoski, J.T., Hilton, D.R., 2004. Climate variability in the Botswana Kalahari from the late Pleistocene to the present day. Geophysical Research Letters 31.

Klotz, S., Guiot, J., Mosbrugger, V., 2003. Continental European Eemian and early Würmian climate evolution: comparing signals using different quantitative reconstruction approaches based on pollen. Global and Planetary Change 36, 277-294.

Kühl, N., Gebhardt, C., Litt, T., Hense, A., 2002. Probability density functions as botanical-climatological transfer functions for climate reconstruction. Quaternary Research 58, 381-392.

Kulongoski, J.T., Hilton, D.R., 2004. Climate variability in the Botswana Kalahari from the late Pleistocene to the present day. Geophysical Research Letters 31.

Kutzbach, J.E., 1981. Monsoon climate of the early Holocene: climate experiment with the Earth's orbital parameters for 9000 years ago. Science 214, 59-61.

Kutzbach, J.E., Street-Perrott, F.A., 1985. Milankovitch forcing of fluctuations in the level of tropical lakes from 18 to 0 kyr BP. Nature 317, 130-134.

Lee-Thorp, J.A., Holmgren, K., Lauritzen, S.-E., Linge, H., Moberg, A., Partridge, T.C., Stevenson, C., Tyson, P.D., 2001. Rapid climate shifts in the southern African interior throughout the mid- to late Holocene. Geophysical Research Letters 28, 4507-4510.

Li, J., Zeng, Q., 2002. A unified monsoon index. Geophys. Res. Lett. 29, 1274.

Liu, Z., Kutzbach, J., Otto-Bliesner, B., Shields, C., Li, L., 2003. Coupled climate simulation of the evolution of global monsoons in the Holocene. Journal of Climate 16, 2472-2490.

Marzin, C., Braconnot, P., 2009. Variations of Indian and African monsoons induced by insolation changes at 6 and 9.5 kyr BP. Climate Dynamics 33, 215-231.

McCormac, F.G., Hogg, A.G., Blackwell, P.G., Buck, C.E., Higham, T.F.G., Reimer, P.J., 2004. SHCal04 Southern Hemisphere Calibration, 0-11.0 Cal Kyr BP. Radiocarbon 46, 1087-1092.

Meadows, M.E., 2001. The role of Quaternary environmental change in the evolution of landscapes: case studies from southern Africa. CATENA 42, 39-57.

Mucina, L., Rutherford, M.C., 2006. The vegetation of South Africa, Lesotho and Swaziland. Strelitzia 19. South African National Biodiversity Institute, Pretoria.

Norström, E., Scott, L., Partridge, T.C., Risberg, J., Holmgren, K., 2009. Reconstruction of environmental and climate changes at Braamhoek wetland, eastern escarpment South Africa, during the last 16,000 years with emphasis on the Pleistocene-Holocene transition. Palaeogeography, Palaeoclimatology, Palaeoecology 271, 240-258.

Phillips, S.J., Anderson, R.P., Schapire, R.E., 2006. Maximum entropy modeling of species geographic distributions. Ecological Modelling 190, 231-259.

Reimer, P.J., Baillie, M.G.L., Bard, E., Bayliss, A., J W Beck, J.W., Blackwell, P.G., Bronk Ramsey, C., Buck, C.E., Burr, G.S., Edwards, R.L., Friedrich, M., Grootes, P.M., Guilderson, T.P., Hajdas, I., Heaton, T.J., Hogg, A.G., Hughen, K.A., Kaiser, K.F., Kromer, B., McCormac, F.G., Manning, S.W., Reimer, R.W., Richards, D.A., Southon, J.R., Talamo, S., Turney, C.S.M., van der Plicht, J., Weyhenmeyer, C.E., 2009. IntCal09 AND Marine09 radiocarbon calibration curves, 0-50,000 years cal BP. Radiocarbon 4, 1111-1150.

Rutherford, M.S., Westfall, R.H., 1986. Biomes of southern Africa: an objective categorization. Memoirs of the Botanical Survey of South Africa 54, 1-98.

Rutherford, M.C., Mucina, L., Powrie, L.W., 2012. The South African National Vegetation Database: History, development, applications, problems and future. South African Journal of Science 108.

Rutherford, M.C., Powrie, L.W., Midgley, G.F., 2003. ACKDAT: A digital spatial database of distributions of South African plant species and species assemblages. South African Journal of Botany 69, 99-104.

SANBI, 2003. PRECIS (National Herbarium Pretoria (PRE) Computerized Information System) database.

Scheful3, E., Kuhlmann, H., Mollenhauer, G., Prange, M., Patzold, J., 2011. Forcing of wet phases in southeast Africa over the past 17,000 years. Nature 480, 509-512.

Scott, L., 1982. A late Quaternary pollen record from the Transvaal bushveld, South Africa. Quaternary Research 17, 339-370.

Scott, L., 1999. Vegetation history and climate in the Savanna biome South Africa since 190,000 ka: a comparison of pollen data from the Tswaing Crater (the Pretoria Saltpan) and Wonderkrater. Quaternary International 57-8, 215-223.

Scott, L., Holmgren, K., Talma, A.S., Woodborne, S., Vogel, J.C., 2003. Age interpretation of the Wonderkrater spring sediments and vegetation change in the Savanna Biome, Limpopo province, South Africa. South African Journal of Science 99, 484-488.

Scott, L., Neumann, F.H., Brook, G.A., Bousman, C.B., Norström, E., Metwally, A.A., 2012. Terrestrial fossil-pollen evidence of climate change during the last 26 thousand years in southern Africa. Quaternary Science Reviews 32, 100-118.

Scott, L., Thackeray, J.F., 1987. Mulivariate analysis of Late Pleistocene and Holocene pollen spectra from Wonderkrater, Transvaal, South Africa. South African Journal of Science 83, 93-98.

Sinninghe-Damsté, J.S., Verschuren, D., Ossebaar, J., Blokker, J., van Houten, R., van der Meer, M.T.J., Plessen, B., Schouten, S., 2011. A 25,000-year record of climate-induced changes in lowland vegetation of eastern equatorial Africa revealed by the stable carbon-isotopic composition of fossil plant leaf waxes. Earth and Planetary Science Letters 302, 236-246.

Smith, G.F., Van Wyk, B., 2008. Aloes in southern Africa. Struik Publishers, Cape Town.

Sonzogni, C., Bard, E., Rostek, F., 1998. Tropical sea-surface temperatures during the last glacial period: a view based on alkenones in Indian Ocean sediments. Quaternary Science Reviews 17, 1185-1201.

Stager, J.C., Ryves, D.B., Chase, B.M., Pausata, F.S.R., 2011. Catastrophic drought in the Afro-Asian monsoon region during Heinrich event 1. Science 331, 1299-1302.

Stute, M., Talma, A.S., 1998. Glacial temperatures and moisture transport regimes reconstructed from noble gas and δ^{18}O, Stampriet aquifer, Namibia, Isotope Techniques in the Study of Past and Current Environmental Changes in the Hydrosphere and the Atmosphere. IAEA Vienna Symposium 1997, Vienna, pp. 307-328.

Swets, J., 1988. Measuring the accuracy of diagnostic systems. Science 240, 1285-1293.

Talma, A.S., Vogel, J.C., 1992. Late Quaternary paleotemperatures derived from a speleothem from Cango Caves, Cape Province, South Africa. Quaternary Research 37, 203-213.

Thackeray, J.F., 1999. Calibration of temperature indices from a late Quaternary terrestrial sequence at Wonderkrater, South Africa. Quaternary International 57-8, 225-227.

Thomas, D.S.G., Bailey, R., Shaw, P.A., Durcan, J.A., Singarayer, J.S., 2009. Late Quaternary highstands at Lake Chilwa, Malawi: frequency, timing and possible forcing mechanisms in the last 44 ka. Quaternary Science Reviews 28, 526-539.

Tierney, J.E., Russell, J.M., Huang, Y., Damste, J.S.S., Hopmans, E.C., Cohen, A.S., 2008. Northern Hemisphere controls on tropical southeast African climate during the past 60,000 years. Science 322, 252-255.

Tyson, P.D., Preston-Whyte, R.A., 2000. The Weather and Climate of Southern Africa. Oxford University Press, Cape Town.

Table 1. Summary of the modelling results. A triangle indicates that the pollen-type was used in the reconstruction of the climatic variable, a black triangle means that pollen-type require high values of the considered variable and a white triangle indicates low values.

Fig.1. Map of the major atmospheric and oceanic circulation systems and convergences zones (the Intertropical Convergence Zone (ITCZ), the Congo Air Boundary (CAB) and the Angola-Benguela Front (ABF)), rainfall seasonality (shading) and the primary sites considered: (1) Wonderkrater (Scott et al, 2003), (2) Cold Air Cave (Holmgren et al., 2003; Lee-Thorp et al., 2001), (3) MD96-2048 marine core (Sonzogni et al., 1998, Bard et al., 1997), (4) MD79257 marine core, Limpopo River (Dupont et al., 2011), (5) GeoB9307-3 marine core (Schefuss et al., 2011), (6) Lake Malawi (Castañeda et al., 2007), (7) Lake Tanganyika (Tierney et al., 2008), (8) Lake Challa (Sinninghe-Damsté et al., 2011).

Fig.2. Biomes of southern Africa with the sites of (1) Wonderkrater (Scott et al., 2003), (2) Cold Air Cave (Holmgren et al., 2003), (3) MD96-2048 marine core (Sonzogni et al., 1998, Bard et al., 1997) shown.

Fig.3. Maps of climatic variables (temperatures during the warmest quarter (TWarmQ), temperatures during the coldest quarter (TCQ), precipitations durig the driest quarter (PDryQ) and precipitations during the wettest quarter (PWetQ)) reconstructed for this study.

Fig.4. Age-depth model calculated from radiocarbon ages selected by Scott et al. (2003)

Fig.5. Outline of the species selection method applied in this paper.

Fig.6. Effect of the weighting method applied on the distribution of Ericaceae as function of TWarmQ. Frequency reflect the number of pixels, grey bars show the distribution of TWarmQ over the study area, black bars show the occurrences of Ericaceae, solid line represent the unweighted *pdf* of Ericaceae and the dashed line represent the *pdf* after the weighting method.

Fig.7. (a) PWetQ requirements variability of Capparaceae. Thick black solid line: *pdf*s of the whole dataset of Capparaceae (vertical exaggeration x10), blue lines: *pdf*s of species requiring wet environment, yelow lines: *pdf*s of species requiring dry environment. (b) Species selection method for Capparaceae. Dotted line: *pdf* of the whole dataset of Capparaceae, shaded area: resulting *pdf* of the assemblage during the early Holocene, dashed line: *pdf* of Capparaceae after species selection method (species with the probability to be found in the assemblage is lower than 0.2 are removed).

Fig.8. Comparison between the reconstructed TwarmQ (a), PWetQ (c), without the species selection method and the reconstructed TWarmQ (b), PWetQ (d), with the species selection method. The values for modern TWarmQ and PWetQ are indicated with a dashed line. Grey shaded area indicates 1-sigma uncertainties.

Fig.9. Comparison between the reconstructed temperatures during the coldest quarter (b), temperatures during the warmest quarter (c), precipitation during the driest quarter (e) and the precipitation during the wettest quarter (f) from Wonderkrater in this paper with the PCA-derived temperature (a) and humidity (d) indices from Scott et al., (2003). Selected taxa from the original pollen diagram (g) from Scott et al., 2003 is also shown along with and the calculated modern climate

values ,dashed line (Hijmans et al., 2005) in b, c, e and f. Grey shaded area indicates 1-sigma uncertainties.

Fig.10. Comparison of Wonderkrater reconstructions (smoothed) for temperatures during the warmest quarter (h), temperatures during the coldest quarter (i), precipitation during the wettest quarter (j) with records from the GRIP ice core from Greenland (a; Shackleton et al., 2004), Lake Challa (b; Sinninghe-Damsté et al., 2011), Lake Malawi (c; Castañeda et al., 2007), the Zambezi Basin (d; Schefuß et al., 2011), Lake Tanganyika (e; Tierney et al., 2008), Cold Air Cave (f; Lee-Thorp et al., 2001), Mozambique Channel (g; Sonzogni et al., 1998, Bard et al., 1997), the humidity index reconstruction at Wonderkrater (k; Scott et al., 2003) and the insolation curves (l,m; Berger & Loutre, 1991).

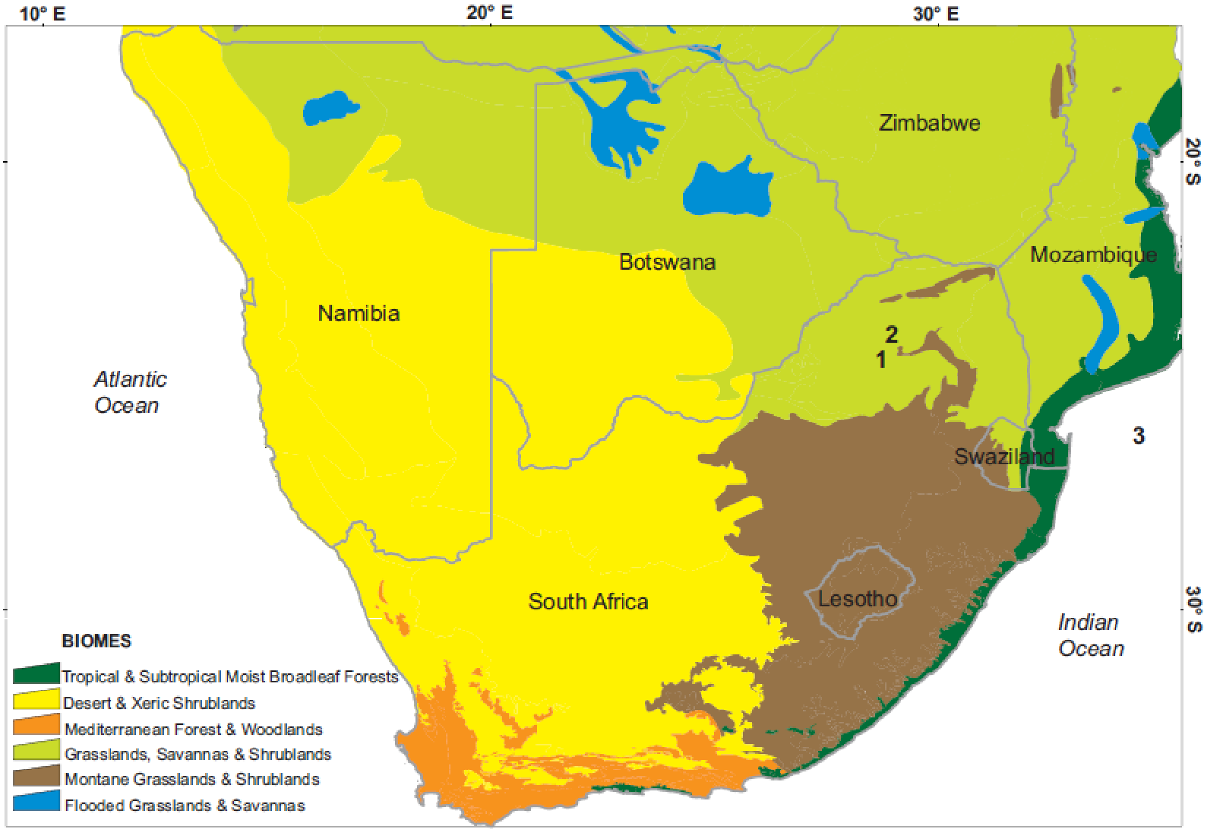
10° E
20° E
30° E
20° S
30° S
Zimbabwe
Botswana
Mozambique
Namibia
Atlantic Ocean
2
1
3
Swaziland
South Africa
Lesotho
Indian Ocean
BIOMES
Tropical & Subtropical Moist Broadleaf Forests
Desert & Xeric Shrublands
Mediterranean Forest & Woodlands
Grasslands, Savannas & Shrublands
Montane Grasslands & Shrublands
Flooded Grasslands & Savannas

Fig. 1

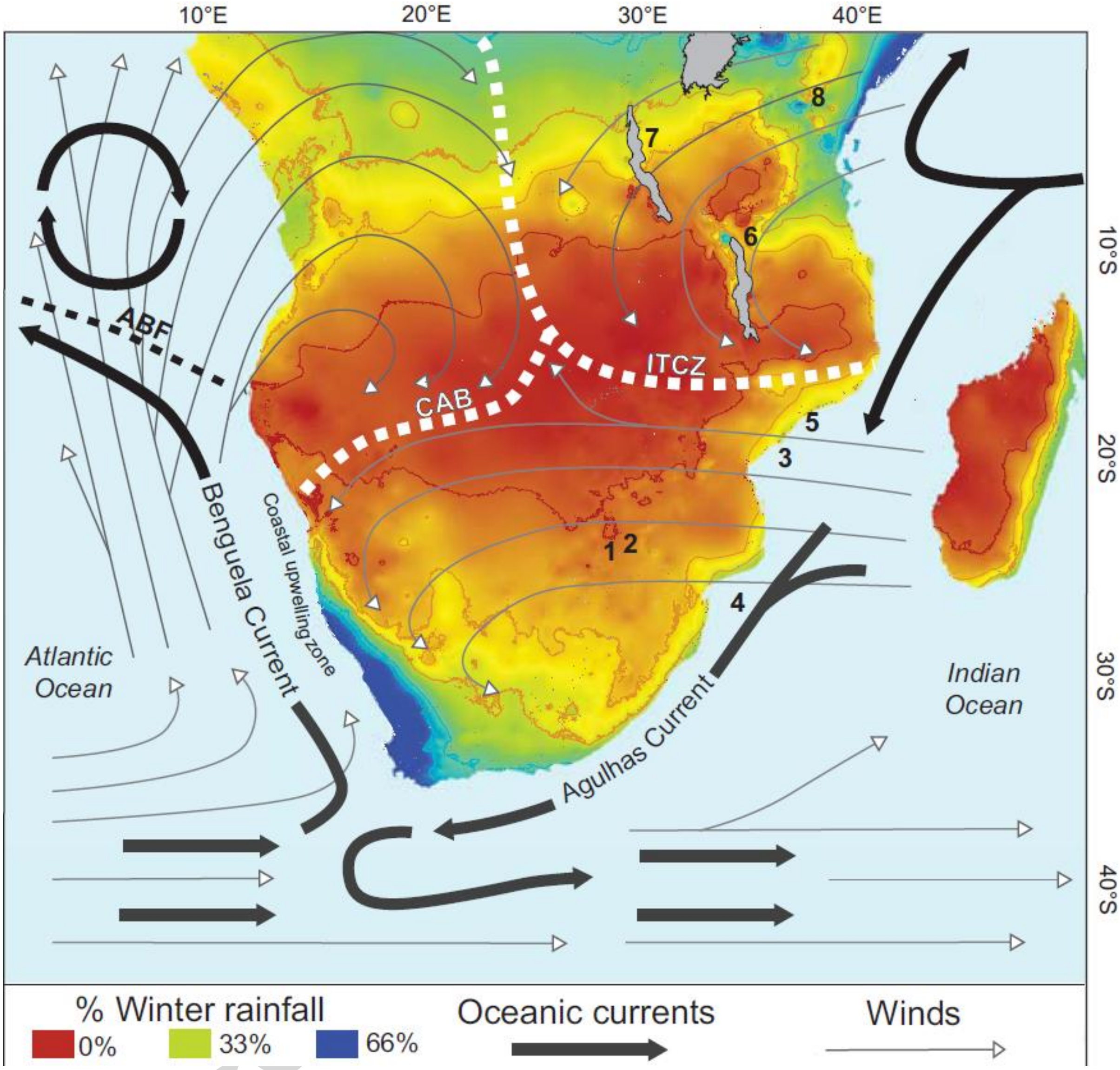
10°E
20°E
30°E
40°E
10°S
20°S
30°S
40°S
ABF
CAB
ITCZ
1
2
3
4
5
6
7
8
Benguela Current
Coastal upwelling zone
Agulhas Current
Atlantic Ocean
Indian Ocean
% Winter rainfall
0%
33%
66%
Oceanic currents
Winds

Fig. 2

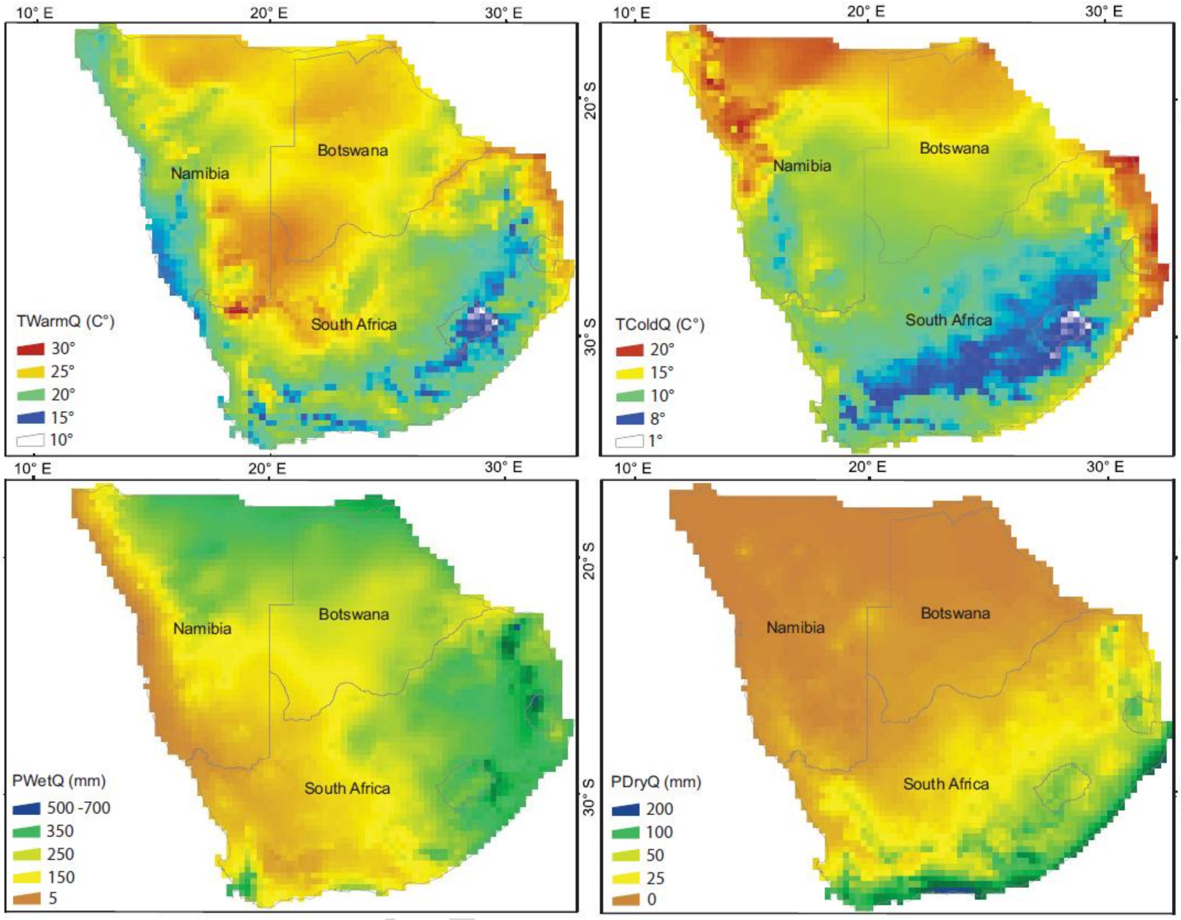
10° E
20° E
30° E
20° S
30° S
Namibia
Botswana
South Africa
TWarmQ (C°)
30°
25°
20°
15°
10°
TColdQ (C°)
20°
15°
10°
8°
1°
PWetQ (mm)
500 -700
350
250
150
5
PDryQ (mm)
200
100
50
25
0

Fig. 3

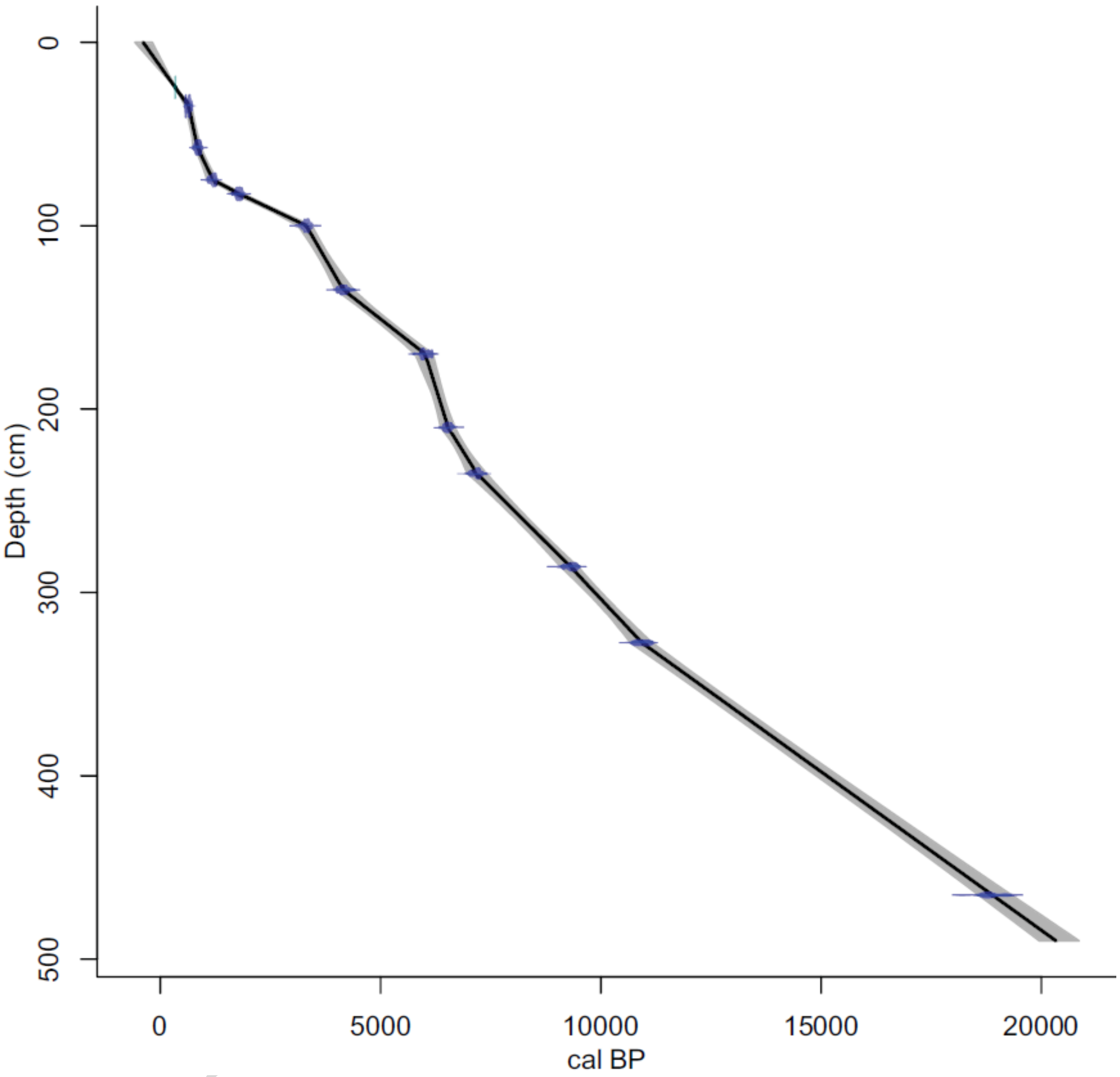

Fig. 4

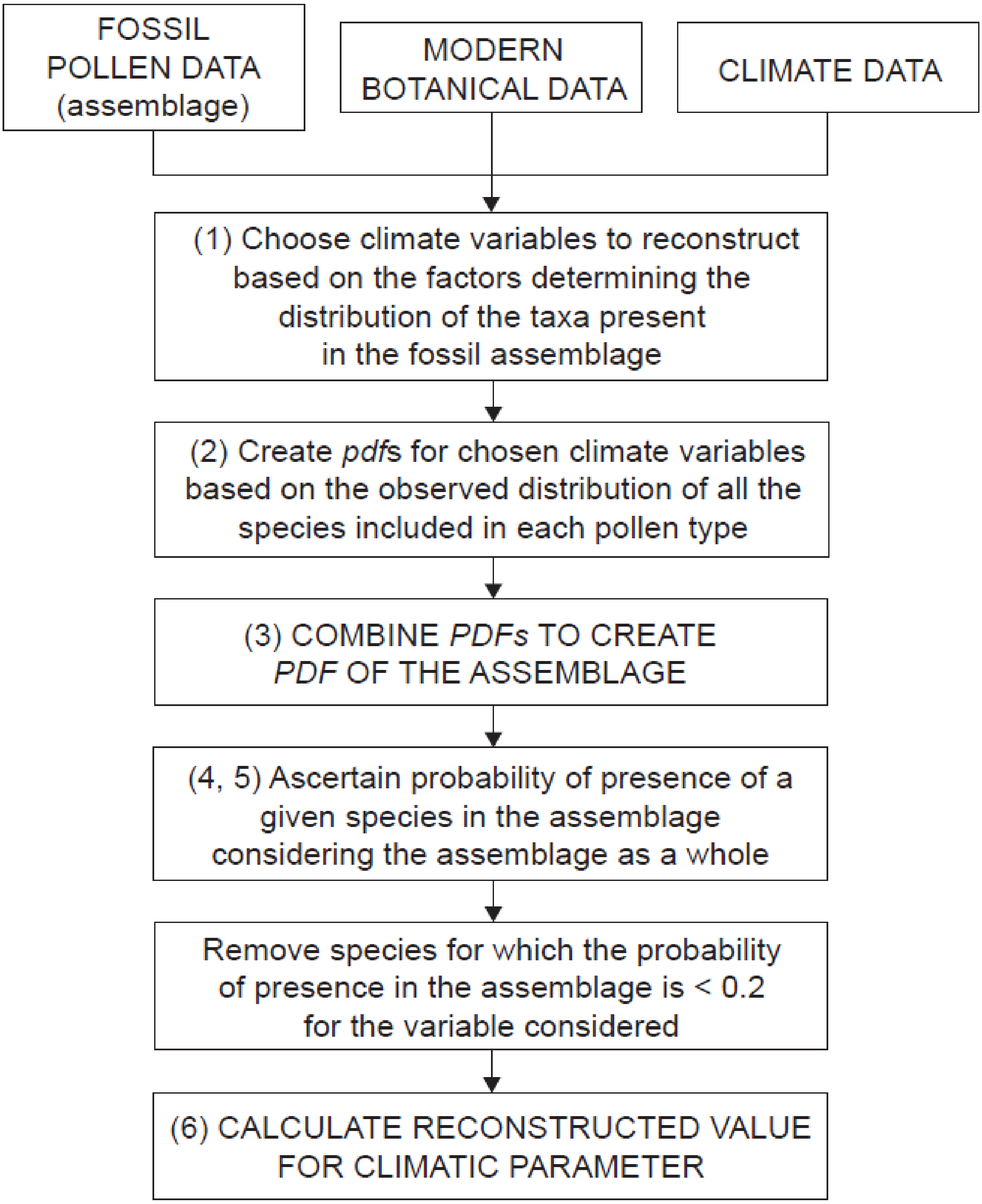
FOSSIL POLLEN DATA (assemblage)
MODERN BOTANICAL DATA
CLIMATE DATA
(1) Choose climate variables to reconstruct based on the factors determining the distribution of the taxa present in the fossil assemblage
(2) Create *pdf*s for chosen climate variables based on the observed distribution of all the species included in each pollen type
(3) COMBINE *PDFs* TO CREATE *PDF* OF THE ASSEMBLAGE
(4, 5) Ascertain probability of presence of a given species in the assemblage considering the assemblage as a whole
Remove species for which the probability of presence in the assemblage is < 0.2 for the variable considered
(6) CALCULATE RECONSTRUCTED VALUE FOR CLIMATIC PARAMETER

Fig. 5

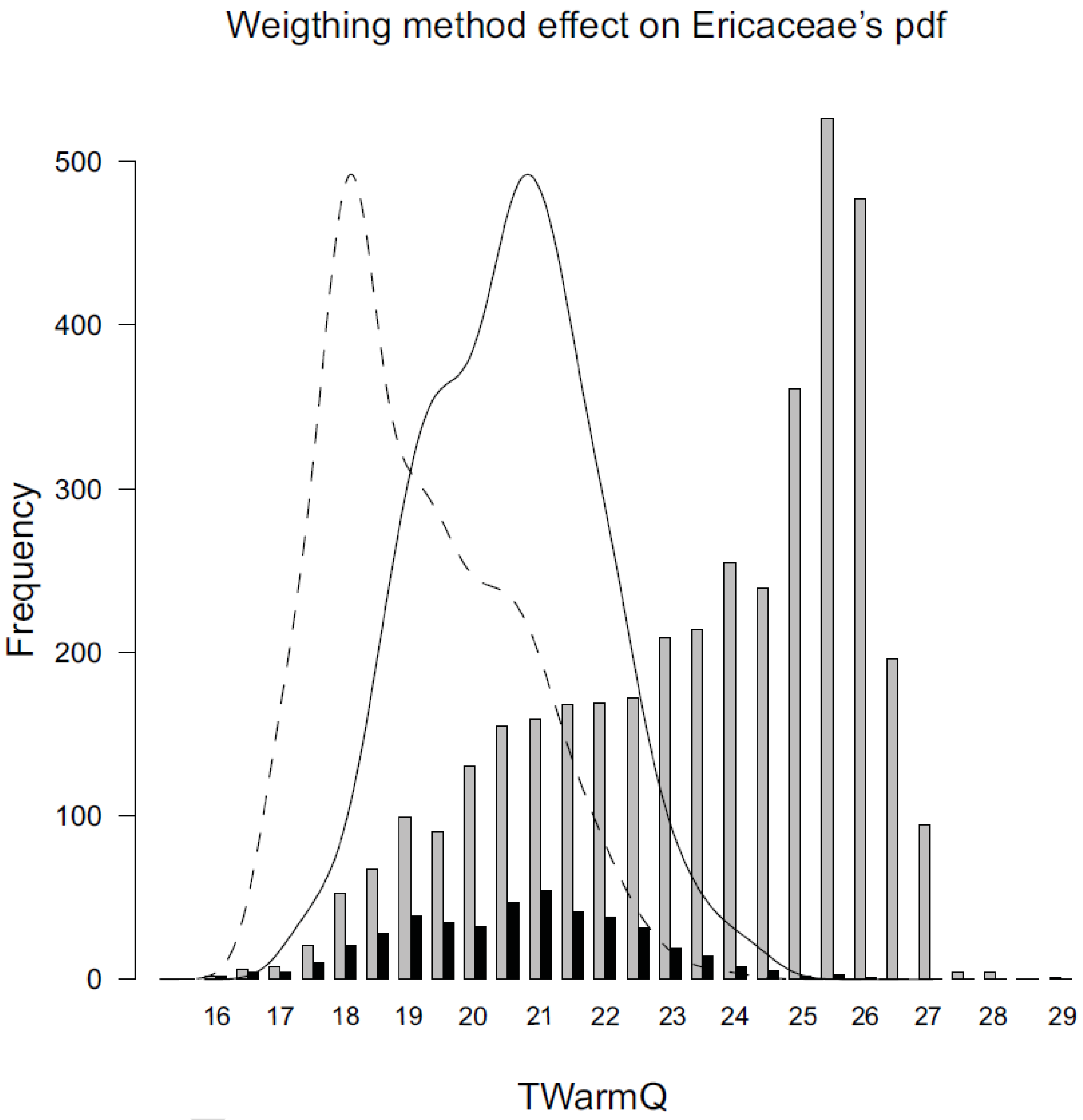
Weigthing method effect on Ericaceae's pdf
Frequency
0
100
200
300
400
500
16
17
18
19
20
21
22
23
24
25
26
27
28
29
TWarmQ

Fig. 6

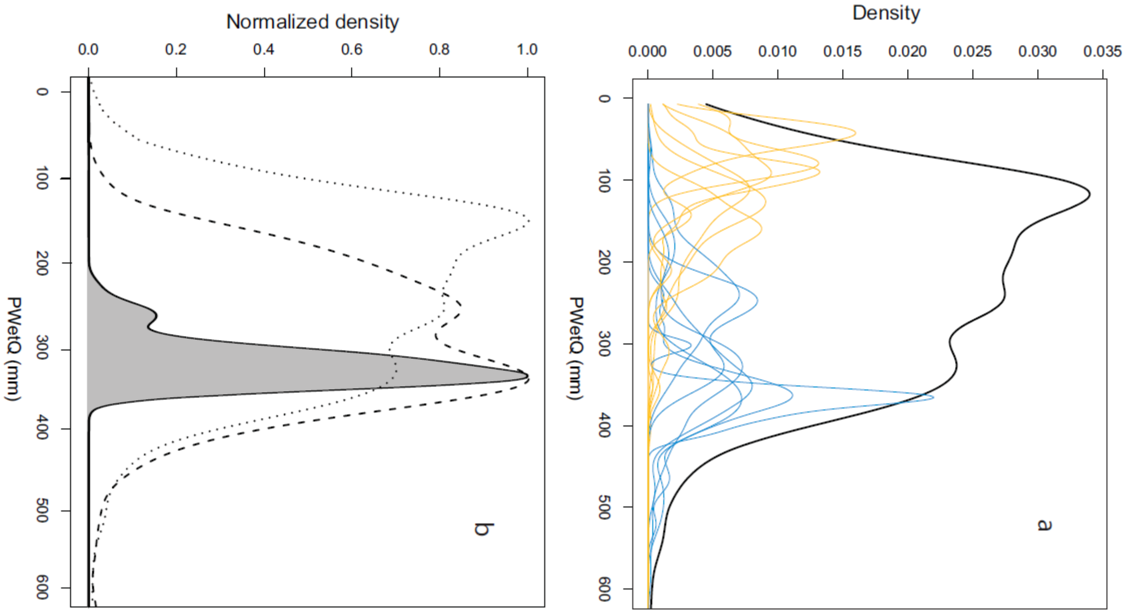
Normalized density
0.0
0.2
0.4
0.6
0.8
1.0
PWetQ (mm)
0
100
200
300
400
500
600
b
Density
0.000
0.005
0.010
0.015
0.020
0.025
0.030
0.035
PWetQ (mm)
0
100
200
300
400
500
600
a

Fig. 7

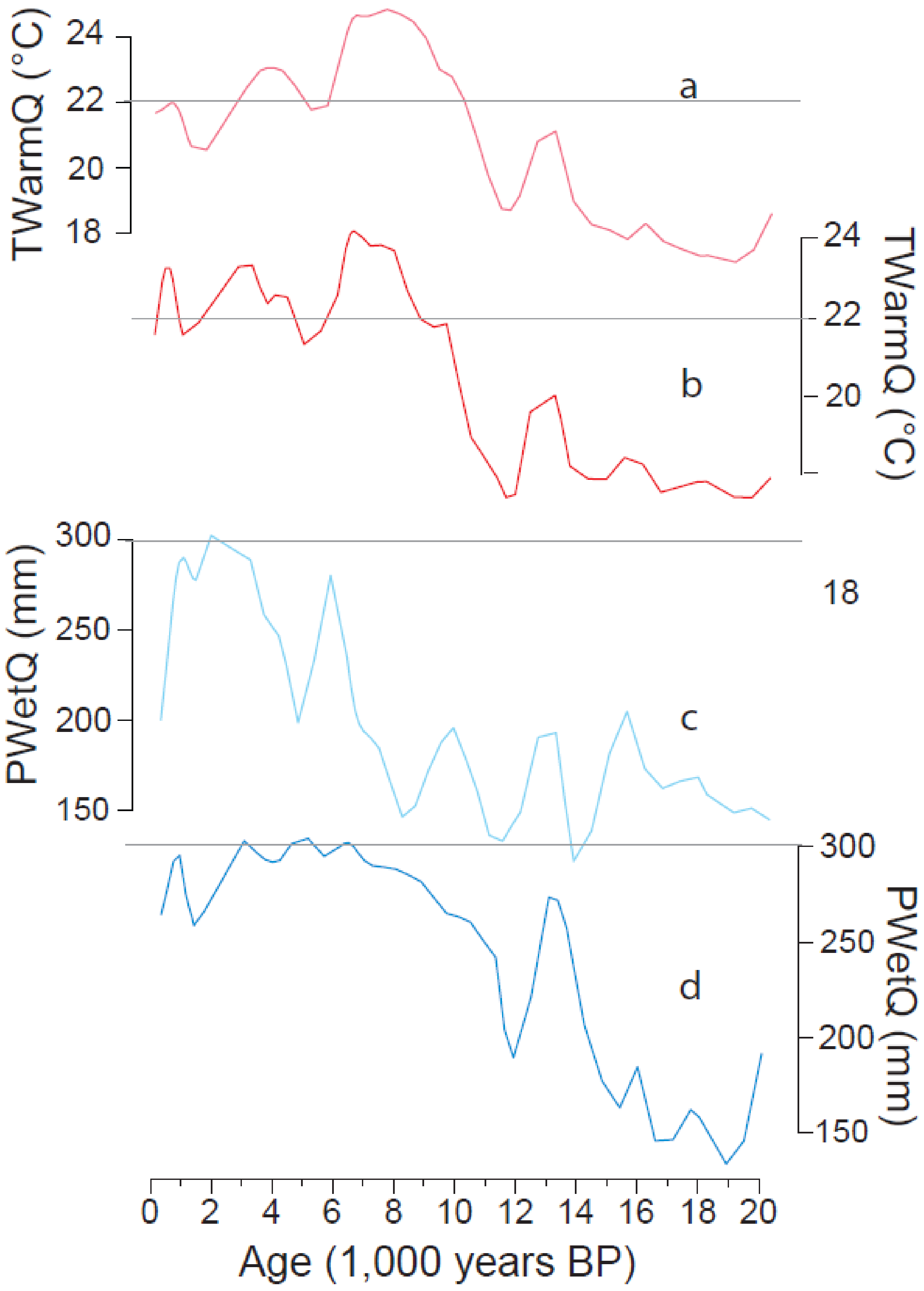
TWarmQ (°C)
24
22
20
18
a
24
22
20
18
TWarmQ (°C)
b
PWetQ (mm)
300
250
200
150
c
300
250
200
150
PWetQ (mm)
d
0
2
4
6
8
10
12
14
16
18
20
Age (1,000 years BP)

Fig. 8

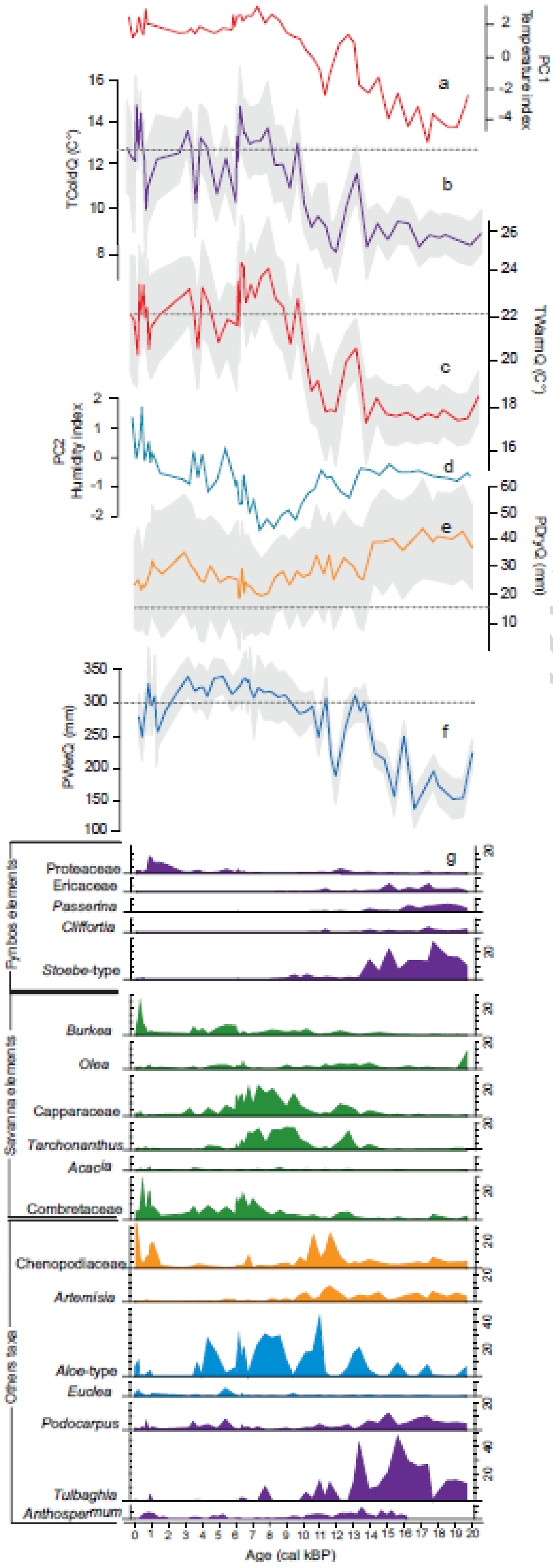
PC1
Temperature index
2
0
-2
-4
a
TColdQ (C°)
16
14
12
10
8
b
26
24
22
20
18
16
TWarmQ (C°)
c
PC2
Humidity index
2
1
0
-1
-2
d
60
50
40
30
20
10
PDryQ (mm)
e
PWetQ (mm)
350
300
250
200
150
100
f
g
Fynbos elements
Proteaceae
Ericaceae
Passerina
Cliffortia
Stoebe-type
Savanna elements
Burkea
Olea
Capparaceae
Tarchonanthus
Acacia
Combretaceae
Others taxa
Chenopodiaceae
Artemisia
Aloe-type
Euclea
Podocarpus
Tulbaghia
Anthospermum
20
40
0 1 2 3 4 5 6 7 8 9 10 11 12 13 14 15 16 17 18 19 20
Age (cal kBP)

Fig. 9

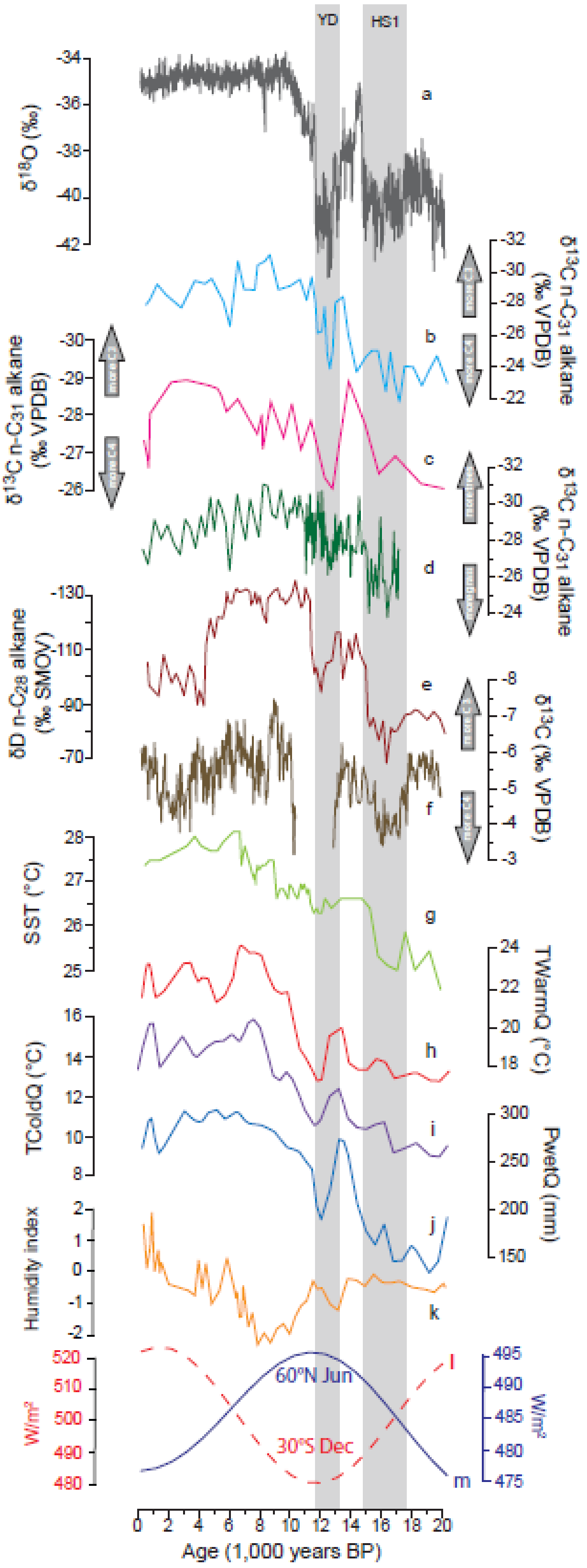
YD
HS1
δ18O (‰)
-34
-36
-38
-40
-42
a
δ13C n-C31 alkane (‰ VPDB)
-32
-30
-28
-26
-24
-22
b
δ13C n-C31 alkane (‰ VPDB)
-30
-29
-28
-27
-26
c
δ13C n-C31 alkane (‰ VPDB)
-32
-30
-28
-26
-24
d
δD n-C28 alkane (‰ SMOV)
-130
-110
-90
-70
e
δ13C (‰ VPDB)
-8
-7
-6
-5
-4
-3
f
SST (°C)
28
27
26
25
g
TWarmQ (°C)
24
22
20
18
h
TColdQ (°C)
16
14
12
10
8
i
PwetQ (mm)
300
250
200
150
j
Humidity index
2
1
0
-1
-2
k
W/m²
520
510
500
490
480
l
60°N Jun
30°S Dec
W/m²
495
490
485
480
475
m
0
2
4
6
8
10
12
14
16
18
20
Age (1,000 years BP)

Fig. 10

Table 1

	Pollen-type	Nb of species	AUC	Temperature		Moisture	
				TColdQ	TWarmQ	PDryQ	PWetQ
Fynbos elements	Ericaceae	124	0.9	▽	▽		
	Cliffortia	29	0.92	▽	▽		
	Proteaceae	96	0.89	▽	▽		
	Passerina	10	0.91	▽	▽		
	Stoebe	5	0.94	▽	▽	▽	▽
Savanna elements	Combretaceae	25	0.82	▲	▲	▲	▲
	Burkea	1	0.91	▲	▲	▲	▲
	Capparaceae	27	0.68	▲	▲	▲	▲
	Tarchonanthus	7	0.83	▲	▲	▲	▲
	Spirostachys	1	0.9	▲	▲	▲	▲
	Acacia	49	0.7	▲	▲	▲	▲
Others taxa	*Podocarpus*	4	0.93	▽	▽	▲	
	Artemisia	1	0.87	▽	▽		
	Chenopodiaceae	31	0.73		▽		▽
	Anthospermum	14	0.82		▽	▲	
	Olea	11	0.85		▽	▲	
	Euclea	17	0.77	▲		▲	▲
	Aloe	42	0.78			▲	▲

Highlights

Quantitative estimates of climate at a key South Africa site over the past 20 kyr

Reconstructed trends show strong link with regional sea-surface temperatures

Reconstructions indicate interhemispheric synchrony in the African tropics

Results do not support hypothesis of precessional forcing of tropical African climate

Highlights a promising technique for analyzing palaeobotanical data in the region